THE JOURNAL OF BIOLOGICAL CHEMISTRY VOL. 286, NO. 36, pp. 31297–31307, September 9, 2011

Physical Association of *Arabidopsis* Hypersensitive Induced Reaction Proteins (HIRs) with the Immune Receptor RPS2*[S]

Received for publication, December 13, 2010, and in revised form, July 7, 2011 Published, JBC Papers in Press, July 13, 2011, DOI 10.1074/jbc.M110.211615

Yiping Qi[‡1], Kenichi Tsuda[‡], Le V. Nguyen[‡], Xia Wang[§], Jinshan Lin[§], Angus S. Murphy[§], Jane Glazebrook[‡], Hans Thordal-Christensen[¶], and Fumiaki Katagiri[‡2]

From the [‡]Department of Plant Biology, Microbial and Plant Genomics Institute, University of Minnesota, St. Paul, Minnesota 55108, the [§]Department of Horticulture, Purdue University, West Lafayette, Indiana 47907-2010, and [¶]Plant and Soil Science, Department of Agriculture and Ecology, Faculty of Life Sciences, University of Copenhagen, Thorvaldsensvej 40, DK-1871 Frederiksberg C, Denmark

Arabidopsis **RPS2 is a typical nucleotide-binding leucine-rich repeat resistance protein, which indirectly recognizes the bacterial effector protein AvrRpt2 and thereby activates effector-triggered immunity (ETI). Previously, we identified two hypersensitive induced reaction (AtHIR) proteins, AtHIR1 (At1g09840) and AtHIR2 (At3g01290), as potential RPS2 complex components. AtHIR proteins contain the stomatin/prohibitin/flotillin/HflK/C domain (also known as the prohibitin domain or band 7 domain). In this study, we confirmed that AtHIR1 and AtHIR2 form complexes with RPS2 in *Arabidopsis* and *Nicotiana benthamiana* using a pulldown assay and fluorescence resonance energy transfer (FRET) analysis. *Arabidopsis* has four HIR family genes (*AtHIR1–4*). All AtHIR proteins could form homo- and hetero-oligomers *in vivo* and were enriched in membrane microdomains of the plasma membrane. The mRNA levels of all except *AtHIR4* were significantly induced by microbe-associated molecular patterns, such as the bacterial flagellin fragment flg22. *Athir2-1* and *Athir3-1* mutants allowed more growth of *Pto* DC3000 AvrRpt2, but not *Pto* DC3000, indicating that these mutations reduce RPS2-mediated ETI but do not affect basal resistance to the virulent strain. Overexpression of *AtHIR1* and *AtHIR2* reduced growth of *Pto* DC3000. Taken together, the results show that the AtHIR proteins are physically associated with RPS2, are localized in membrane microdomains, and quantitatively contribute to RPS2-mediated ETI.**

Plants have two major types of immune receptors that perceive signals from pathogens and initiate defense induction. The first type are called pattern recognition receptors. They recognize pathogen- or microbe-associated molecular patterns (MAMPs)[3] and initiate pathogen-associated molecular pattern- or pattern-triggered immunity (PTI) (1–3). A well studied pattern recognition receptor is the *Arabidopsis* FLS2, which recognizes flg22, a 22-amino acid peptide of bacterial flagellin (4, 5). The second type are called resistance (R) proteins. They recognize specific pathogen effector proteins and trigger effector-triggered immunity (ETI) (2), which is also known as gene-for-gene resistance (6). The majority of plant R proteins belong to the nucleotide-binding leucine-rich repeat (NB-LRR) class (7). Based on differences in N-terminal sequences, the NB-LRR family can be divided into two subclasses: coiled coil-NB-LRR and Toll and interleukin-1 region-NB-LRR (7). The *Arabidopsis* R proteins RPS2 and RPM1 belong to the coiled coil-NB-LRR subclass (8–11). Many Gram-negative bacterial pathogens deliver into plant cells a number of type III effector proteins, which target specific host proteins or DNAs for perturbation of PTI (12) and acquisition of nutrients (13). Plant R proteins have evolved to recognize pathogen effectors through either directly binding to the effectors or binding to certain host proteins that are targets of pathogen effectors (7). The phenomenon in the latter case can be explained by the "guard hypothesis": R proteins "guard" effector-targeted plant proteins, called "guardees"; R proteins detect modifications of their guardees caused by the effectors and trigger signaling to induce ETI (7). For example, RPS2 binds the guardee RIN4 and triggers ETI when RIN4 is cleaved by the bacterial effector AvrRpt2 (14, 15).

Plant cells undergoing ETI often show a hypersensitive response (HR), which is a programmed cell death phenomenon thought to prevent biotrophic pathogens from spreading (16, 17). Some members of the hypersensitive induced reaction (*HIR*) gene family are transcriptionally induced in the cells undergoing HR (18). *HIR* family members have been isolated from multiple plant species, including tobacco (19), maize (18), barley (20), pepper (21), and wheat (22). Overexpression of a pepper *HIR* gene (*CaHIR1*) in *Arabidopsis* caused enhanced disease resistance to *Pseudomonas syringae* pv. *tomato* (*Pto*) DC3000 (21, 23). However, the mechanism of *HIR* gene involvement in plant immunity is not clear.

The *HIR* family genes encode proteins of ~30 kDa that contain the stomatin/prohibitin/flotillin/HflK/C (SPFH) domain, also known as the prohibitin domain (24, 25) or band 7 domain.

* This work was supported by Grants IOS-0419648 (*Arabidopsis* 2010 Program) and MCB-0918908 from the National Science Foundation (to F. K.).

[S] The on-line version of this article (available at http://www.jbc.org) contains supplemental Figs. S1–S5 and Table S1.

[1] Supported by a Hamm Memorial Graduate Student fellowship and a PBS doctoral dissertation fellowship from the University of Minnesota.

[2] To whom correspondence should be addressed: Dept. of Plant Biology, Microbial and Plant Genomics Institute, University of Minnesota, 1500 Gortner Ave., St. Paul, MN 55108. Fax: 612-624-6264; E-mail: katagiri@umn.edu.

[3] The abbreviations used are: MAMP, microbe-associated molecular pattern; ETI, effector-triggered immunity; PM, plasma membrane; SPFH, stomatin/prohibitin/flotillin/HflK/C; PTI, pattern-triggered immunity; NB-LRR, nucleotide-binding leucine-rich repeat; R, resistance; CFP, cyan fluorescent protein; DRM, detergent-resistant microdomain; HR, hypersensitive response; HPB, HA-PreScission-Biotin; DSP, dithiobis(succinimidyl propionate); TTSS, type III secretion system.

The SPFH domain-containing proteins are present in divergent species, including both prokaryotes and eukaryotes (26–28). They are localized to a variety of cellular membranes, including plasma membrane (PM), Golgi, mitochondria, endoplasmic reticulum, and lipid droplets (25, 26, 29, 30). They have been implicated in many functions, including ion channel regulation, microdomain formation, membrane protein chaperoning, vesicle trafficking, and membrane-cytoskeletal connection (25, 26, 29, 31, 32). Plant prohibitin proteins are involved in mitochondrial biogenesis and nitric oxide-mediated responses (33, 34). Although the SPFH domain-containing proteins are involved in many biological processes, the molecular basis of their functions remains unclear.

We have been studying plant R protein function, with a focus on the *Arabidopsis* RPS2 protein. To discover more proteins that physically associate with RPS2, we recently developed a protein complex purification method and used it to identify putative RPS2 complex components (35). Two *Arabidopsis* HIR proteins (encoded by At1g69840 and At3g01290) were co-purified with RPS2. Here, we present a biochemical and genetic study of the *Arabidopsis HIR* (*AtHIR*) gene family, which suggests that at least some AtHIR proteins are physically associated with RPS2 and involved in RPS2-mediated ETI.

EXPERIMENTAL PROCEDURES

Constructs—For HA-PreScission-Biotin (HPB) fusion constructs, the cDNA sequences (without the stop codon) of *RPS2* (At4g26090), *AtHIR1* (At1g69840), *AtHIR2* (At3g01290), *AtHIR3* (At5g51570), and *AtHIR4* (At5g62740) were PCR-amplified using Col-0 (referred to Col hereafter) cDNA as the template, cloned into the entry vector pcr8/GW/TOPO® (Invitrogen), and then moved into the destination vector pMDC32-HPB (35) by LR reactions of the Gateway® cloning technology (Invitrogen) to obtain pMDC32-RPS2-HPB, pMDC32-AtHIR1-HPB, pMDC32-AtHIR2-HPB, pMDC32-AtHIR3-HPB, and pMDC32-AtHIR4-HPB. To make *YFP/CFP-HA* fusion constructs, LR reactions were conducted with the entry clones containing *AtHIR1*, *AtHIR2*, or *RPS2* and destination vectors pEG101 or pEG102 (36), to make pEG101-RPS2-YFP-HA, pEG102-AtHIR1-CFP-HA, and pEG102-AtHIR2-CFP-HA. To make Myc fusion constructs, DNA sequence coding the Myc epitope tag (EQKLISEEDL) was included in the 3′ primers for the PCR amplification of *AtHIR1-Myc*, *AtHIR3-Myc*, and *AtHIR4-Myc* from Col cDNAs. The *AtHIR2* genomic sequence containing the 1.5-kb sequence upstream from its start codon (*proAtHIR2-AtHIR2*) was PCR-amplified from Col genomic DNA. All four sequences were cloned into the entry vector pcr8/GW/TOPO® and then moved into the destination vectors pMDC32 (37) and pEG303 (36) to make pMDC32-AtHIR1-Myc, pMDC32-AtHIR3-Myc, pMDC32-AtHIR4-Myc, and pEG303-proAtHIR2-AtHIR2-Myc. The T7-RIN4 construct was used previously (38). All the primers used are summarized in supplemental Table S1. All the constructs were used to transform *Agrobacterium tumefaciens* GV3101/pMP90.

Plants—All the plants used in this study were the Col genetic background. T-DNA insertion lines, including *Athir1-1* (SALK_088328), *Athir2-1* (SALK_092306), *Athir3-1* (SAIL_823_D07), and WiscDsLox489-492B7, were all obtained from the ABRC stock center. *Athir1-1* was genotyped using primers LBe, LP1, and RP1, and *Athir2-1* was genotyped using primers LBe_Sail, LP2, and RP2. *Athir3-1* was genotyped using primers LBe2, LP3, and RP3 (39). WiscDsLox489-492B7 was genotyped using primers LBe_Wisc, LP4, and RP4. Plant growth conditions were as described in Tsuda *et al.* (40). To make transgenic *p35S-AtHIR1/2/3/4-YFP-HA* plants, *AtHIR1*/2/3/4 cDNAs were cloned into pEG101 vector and delivered to Col plants using the floral dip method (41). Plants *RPS2-HPB-1* and *rps2 rpm1* were described previously (35).

RNA—Total RNA was isolated from plant leaves with TRIzol reagent (Invitrogen). RT-PCR was performed using the Qiagen OneStep RT-PCR kit (Qiagen). The MAMP-treated RNA samples used for quantitative RT-PCR were used in previous work (40). The primer sequences are shown in supplemental Table S1. The experiment was performed and analyzed as described previously (42).

Bacteria—The bacterial strains *Pto* DC3000 and *Pto* DC3000 *hrcC* were cultured in King's B medium with 25 μg/ml rifampicin at room temperature (~25 °C). *Pto* DC3000 carrying *AvrRpm1* (43), *AvrRpt2* (44), or the empty vector pLAFR (45) were cultured in King's B medium with rifampicin (25 μg/ml) and tetracycline (10 μg/ml). Plant growth and *in planta* bacterial growth assays were performed as described in Tsuda *et al.* (40).

Subcellular Localization—Microsomal fractionation was performed as described in Qi and Katagiri (35). Detergent-resistant microdomain (DRM) was prepared as described previously (46).

Agrobacterium-mediated Transient Expression in Nicotiana benthamiana—*Agrobacterium* strains carrying desired constructs were cultured at 28 °C to an A_{600} approximately equivalent to 1. Then each strain was collected by centrifugation at 8000 × *g* for 2 min. The bacterial pellets were resuspended with MES buffer (10 mM MES, pH 5.6, 10 mM $MgCl_2$, 150 μM acetosyringone). For pulldown of AtHIR1-Myc and AtHIR2-Myc by RPS2-HPB or for FRET analysis, the ratio of the *Agrobacterium* strains carrying the *AtHIR* construct, the *RPS2* construct, and the *T7-RIN4* construct was 1:1:4 (the culture suspensions were mixed to reach final concentrations of A_{600} = 0.2, 0.2, and 0.8, respectively). For testing oligomerization, the ratio of *Agrobacteria* containing different *AtHIR* constructs was 1:1 (A_{600} = 0.4 each in this case). The *Agrobacterium* suspension was incubated with agitation at 28 °C for 1–2 h. Then the *Agrobacterium* suspension was hand-infiltrated into well expanded leaves of 4-week-old *N. benthamiana* plants, which were grown under a 16-h light/8-h dark cycle with 60% humidity at 25 °C. The outline borders of the infiltrated areas were marked by a Sharpie pen. Two days after infiltration, infiltrated areas of the leaves were collected for pulldown assays or FRET analysis.

Pulldown Assay—For pulldown using *N. benthamiana* samples, 1 g of each leaf sample was quickly frozen in liquid nitrogen and ground with a mortar and pestle to fine powder. Then 2 ml of Extraction buffer (50 mM HEPES-KOH, pH 7.6, 150 mM NaCl, 1% Nonidet P-40, 0.5% sodium deoxycholate, 1 mM DTT) with protease inhibitors (1 tablet/10 ml Complete Mini®, 1 mM

PMSF, 1 μg/ml leupeptin, 1 μg ml^{-1} pepstatin, 1 μg ml^{-1} E64; all from Roche Applied Science) was added and mixed well. Each ground sample in Extraction buffer (~2 ml) was incubated at 4 °C on a rotator for 30 min for solubilization, followed by centrifugation at 16,000 × *g* at 4 °C for 30 min to obtain protein extracts. Meanwhile, 100 μl per sample of Dynabeads® M-280 was washed with Extraction buffer three times and suspended in 100 μl per sample of Extraction buffer. The protein extracts were mixed with 100 μl of pre-washed Dynabeads® M-280 and incubated on a rotator at 4 °C for 2 h. The streptavidin beads were then washed three times with RIPA buffer 1 (50 mM Tris/HCl, pH 7.4, 150 mM NaCl, 1 mM EDTA, 1% Nonidet P-40, 0.5% sodium deoxycholate, 1 mM PMSF) and three times with RIPA buffer 2 (same as RIPA buffer 1, except that 50 mM (instead of 150 mM) NaCl was used). The bead-captured proteins were eluted by heating the beads in 60 μl of 1× SDS sample buffer at 99 °C for 10 min. Pulldown in *Arabidopsis* was conducted in the same manner as described previously (35), except that only 10 g of leaf tissue for each sample was used.

Protein and Immunoblot—Other protein samples described in this study were prepared by directly grinding 0.2 g of frozen leaf tissue in 400 μl of 2× SDS sample buffer with small mortars and pestles. The tubes containing the extracts were boiled for 6 min and then spun at 16,000 × *g* at room temperature for 10 min. The supernatants were loaded for SDS-PAGE, followed by protein staining and immunoblot analysis as described previously (35). An anti-AtHIR1 antiserum was raised against the peptide "DQSNVAIKETFGKF" using rabbits. The resulting polyclonal antibody was affinity-purified, dissolved in PBS buffer, pH 7.4, at 0.458 mg/ml and used at 1:500 dilution. The antibody production and purification service was provided by GenScript. Other antibodies used were as follows: anti-c-Myc monoclonal antibody (Santa Cruz Biotechnology, clone 9E10) at 1:200 dilution; anti-HA high affinity monoclonal antibody (Roche Applied Science, clone 3F10) at 1:500 dilution; anti-Hsc70 (Hsp73) monoclonal antibody (StressGen) at 1:1000 dilution; anti-RIN4 polyclonal antibody (a gift from Jeff Dangl, University of North Carolina) at 1:5000 dilution; anti-PEN1 polyclonal antibody at 1:1000 dilution (47). The secondary antibodies used were as follows: Stabilized goat anti-rabbit horseradish peroxidase (HRP) conjugate (Pierce) at 1:5000 dilution; goat anti-mouse HRP conjugate (Pierce) at 1:5000 dilution; goat anti-rat IgG-h + I HRP conjugate (Bethyl) at 1:5000 dilution. For detection of HRP, SuperSignal® West Femto maximum sensitivity substrate (Pierce) was used, and images were collected using a chilled CCD camera.

Confocal Microscopy and FRET Analysis—For FRET analysis, *N. benthamiana* leaves expressing both AtHIR1-CFP-HA and RPS2-YFP-HA proteins were cut into ~5 × 5-mm squares and mounted between slides and cover glasses with water. The samples were then excited with either 457 nm laser (for CFP) or 514 nm laser (for YFP), and emission signals were filtered through the CFP (488 nm) and YFP (543 nm) filters, using an Eclipse C1si spectral imaging confocal microscope (Nikon). Four data sets were collected, including CFP excitation and YFP emission, CFP excitation and CFP emission, YFP excitation and YFP emission, and YFP excitation and CFP emission. The normalized FRET signals were calculated from all four data sets using EZ-C1 software (Nikon). For AtHIR1 and AtHIR2 localization, 5-week old rosette leaves of *Arabidopsis* T2 transgenic plants were examined for YFP fluorescence using the same equipment.

RESULTS

Arabidopsis HIR Family Genes and Anti-AtHIR1 Antibody— A BLAST search in the *Arabidopsis* genome revealed four members of the *AtHIR* gene family. They are encoded by *At1g69840*, *At3g01290*, *At5g51570*, and *At5g62740*, which we arbitrarily named *AtHIR1*, *AtHIR2*, *AtHIR3*, and *AtHIR4*, respectively (supplemental Fig. S1*A*). The proteins are ~30 kDa, and the only established conserved motif is the SPFH domain (24, 25). AtHIR1, AtHIR4, and AtHIR2 proteins are most closely related, and the amino acid identity between any pair of the four AtHIR proteins is at least 53% (supplemental Fig. S1). Both AtHIR1 and AtHIR2 proteins were identified as putative RPS2 complex components (35), and thus these two proteins, which have 68% amino acid identity, were given priority in the following studies.

To facilitate biochemical characterization of AtHIR proteins, we produced an antibody against AtHIR1, using a 14-amino acids peptide close to the N terminus of the protein as antigen (supplemental Fig. S1*A*). To test the specificity of the obtained anti-AtHIR1 antibody, all four AtHIR proteins were tagged with a Myc epitope tag at the C terminus and expressed in *N. benthamiana* leaves through *Agrobacterium*-mediated transient expression (48). The extracted total proteins were subjected to immunoblot using an anti-Myc and the anti-AtHIR1 antibodies. As expected, anti-Myc antibody detected all four AtHIR-Myc proteins, and no signal was detected in the negative control sample (supplemental Fig. S2). The anti-AtHIR1 antibody could detect AtHIR1, AtHIR2, and AtHIR4 but not AtHIR3 (supplemental Fig. S2). This is consistent with the fact that the peptide sequence used for raising the anti-AtHIR1 antibody is relatively conserved among AtHIR1, AtHIR2, and AtHIR4 but not AtHIR3 (supplemental Fig. S1*A*). The ratios of band intensities among AtHIR1-Myc, AtHIR2-Myc, and AtHIR4-Myc on the immunoblots were similar between the anti-Myc and anti-AtHIR1 antibodies (supplemental Fig. S2). This suggests that the affinities of anti-AtHIR1 antibody to AtHIR1, AtHIR2, and AtHIR4 are comparable. Protein bands representing SDS-, 2-mercaptoethanol-, and heat-resistant oligomers of AtHIR2-Myc and AtHIR4-Myc were detected as bands of larger molecular weights (supplemental Fig. S2). Treatment with high concentrations (up to 100 mM) of dithiothreitol (DTT) could not disassemble such oligomers to monomers (data not shown), indicating that the formation of such oligomers is not based on disulfide bonds.

Pulldown of AtHIR Proteins by RPS2 in Arabidopsis—To confirm that certain AtHIR proteins are associated with RPS2 in *Arabidopsis*, a pulldown assay was conducted using a plant line transgenically expressing *RPS2-HPB* from the *RPS2* promoter in the *rpm1 rps2* double mutant background (35). HPB-tagged proteins are biotinylated in plant cells and thus can be captured by streptavidin beads (35). Indeed, an AtHIR-related band was detected by anti-AtHIR1 antibody in the pulldown sample from RPS2-HPB plants, but not from negative control *rpm1 rps2* plants (Fig. 1*A*). Because AtHIR1, AtHIR2, and AtHIR4 all can

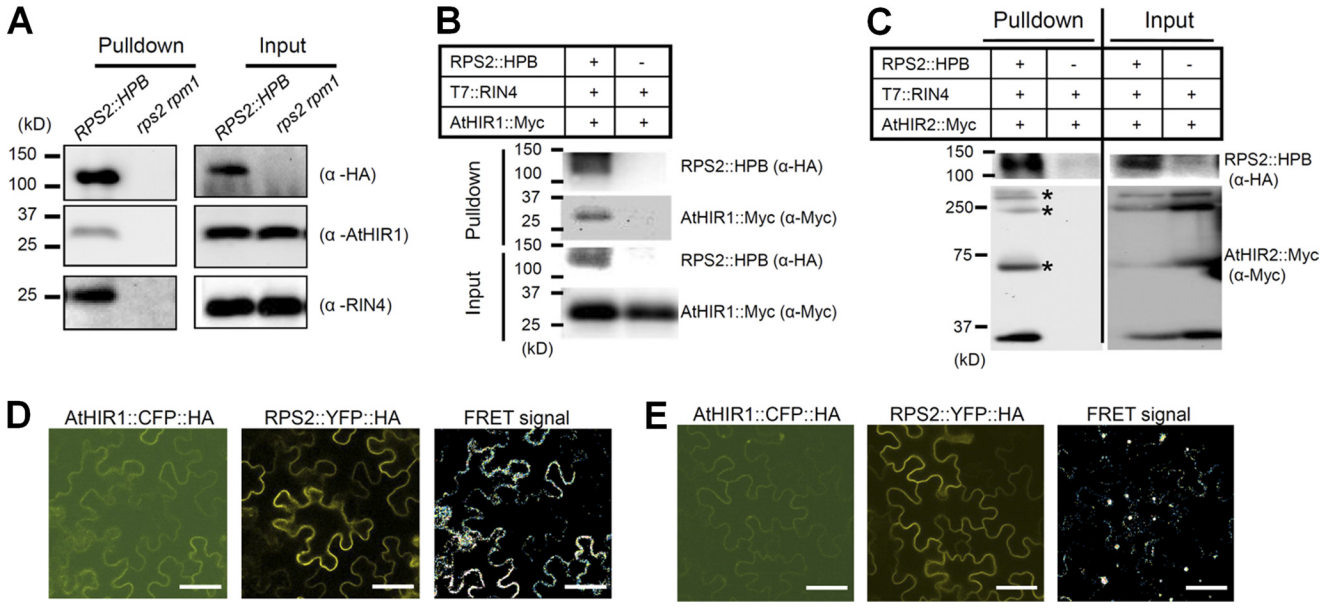

FIGURE 1. **AtHIR1 and AtHIR2 are physically associated with RPS2 *in vivo*.** *A,* AtHIR proteins form complexes with R proteins in *Arabidopsis*. The microsomal fractions from *RPS2-HPB-1 rpm1 rps2* and *rpm1 rps2* were subjected to protein cross-linking with DSP, and the total proteins solubilized from the cross-linked fractions were subjected to pulldown with streptavidin beads. Both input (*right panels*) and pulldown (*left panels*) protein samples were analyzed by immunoblot using anti-HA (α-*HA*), anti-AtHIR1 (α-*AtHIR1*), and anti-RIN4 (α-*RIN4*) antibodies. *B,* AtHIR1-Myc forms a complex with RPS2-HPB in *N. benthamiana*. RPS2-HPB, T7-RIN4, and AtHIR1-Myc were transiently co-expressed in a half-leaf of *N. benthamiana*. As a negative control, T7-RIN4 and AtHIR1-Myc were co-expressed in the other half of the leaf. Both streptavidin bead pulldown samples and input samples were detected by immunoblot using the anti-HA and anti-Myc antibodies. *C,* AtHIR2-Myc forms a complex with RPS2-HPB in *N. benthamiana*. The experiment was done in a similar manner as in *B* except that AtHIR2-Myc, instead of AtHIR1-Myc, was used in co-expression. *D* and *E,* detection of *in vivo* physical association between AtHIR1 and RPS2 by FRET in *N. benthamiana*. AtHIR1-CFP-HA, RPS2-YFP-HA, and T7-RIN4 proteins were co-expressed in *N. benthamiana* leaves, which were used for FRET analysis. The *left panel* shows CFP signal from AtHIR1-CFP-HA. The *middle panel* shows YFP signal from RPS2-YFP-HA. The *right panel* shows FRET signal normalized by the software EZ-C1 3D Option (Nikon, Version 1.00). The experiments of *A–C* were performed twice independently with similar results. Results of *D* and *E* were observed four times and two times, respectively, from six independent samples.

be recognized by this antibody and all of them have very similar sizes, it is not possible to determine which AtHIR protein(s) was pulled down in this experiment. Nevertheless, the data suggest at least one of them can form protein complexes with RPS2 in *Arabidopsis*. The cross-linker dithiobis(succinimidyl propionate) (DSP) was applied in this pulldown assay. AtHIR proteins could not be detected in the pulldown sample from the *RPS2-HPB* plants without applying DSP (data not shown). This is consistent with our previous work that identified both AtHIR1 and AtHIR2 as putative RPS2 complex components when DSP was used for cross-linking the protein complex before purification (35). The requirement for DSP suggests that such physical associations are transient and/or weak and do not survive the stringent wash conditions we used in the study (1% Nonidet P-40, 0.5% sodium deoxycholate). However, DSP cross-linking was not necessary and not used in any other pulldown experiments in this study, in which the proteins were expressed in *N. benthamiana* (see below).

Pulldown of AtHIR1 and AtHIR2 by RPS2 in Vivo—AtHIR1 and AtHIR2 were specifically tested for complex formation with RPS2. AtHIR1-Myc or AtHIR2-Myc were transiently expressed together with T7-RIN4 and RPS2-HPB in *N. benthamiana*, and pulldown of AtHIR1-Myc or AtHIR2-Myc by RPS2-HPB was attempted. For the negative control, RPS2-HPB was not included for co-expression. T7-RIN4 was co-expressed because transiently expressed RPS2 in *N. benthamiana* induces HR (49), and RIN4, as a negative regulator of RPS2, suppresses this HR (50). AtHIR1-Myc was pulled down by streptavidin beads only when RPS2-HPB was co-expressed (Fig. 1*B*), which indicates the formation of an AtHIR1-Myc-RPS2-HPB protein complex in *vivo*. AtHIR2-Myc was again found to form SDS-, 2-mercaptoethanol-, and heat-resistant oligomers, and the monomer and oligomers were pulled down by RPS2-HPB (Fig. 1*C*), indicating that all the forms of AtHIR2 could form complexes with RPS2 *in vivo*.

Confirmation of AtHIR1-RPS2 Association in Vivo by Fluorescence Resonance Energy Transfer (FRET)—FRET was applied to detect physical associations between AtHIR1 or AtHIR2 and RPS2. For FRET, two kinds of fluorophores are required as follows: the donor fluorophore A with excitation and emission wave lengths, λ_{exA} and λ_{emA}, and the acceptor fluorophore B with excitation and emission wave lengths, λ_{exB} and λ_{emB}, where $\lambda_{exA} < \lambda_{emA} \sim \lambda_{exB} < \lambda_{emB}$. When fluorophores A and B are located close to each other, typically within 7 nm, FRET between the two fluorophores can be observed as an excitation at λ_{exA} yields an emission at λ_{emB} (51). CFP and YFP are commonly used as fluorophores A and B, respectively, in a FRET analysis (52). We tagged AtHIR1 and AtHIR2 with CFP-HA to make AtHIR1-CFP-HA and AtHIR2-CFP-HA, and RPS2 with YFP-HA to make RPS2-YFP-HA. To test an *in vivo* association between AtHIR1 and RPS2, AtHIR1-CFP-HA was transiently expressed together with RPS2-YFP-HA and T7-RIN4 in *N. benthamiana,* and FRET analysis was conducted. A FRET signal was clearly detected (Fig. 1, *D* and *E*). This observation indicates that AtHIR1 and RPS2 proteins indeed form a complex together *in vivo*. Considering the short distance between the fluorophores that is required for FRET, it is likely that the physical association between AtHIR1 and RPS2 is direct contact.

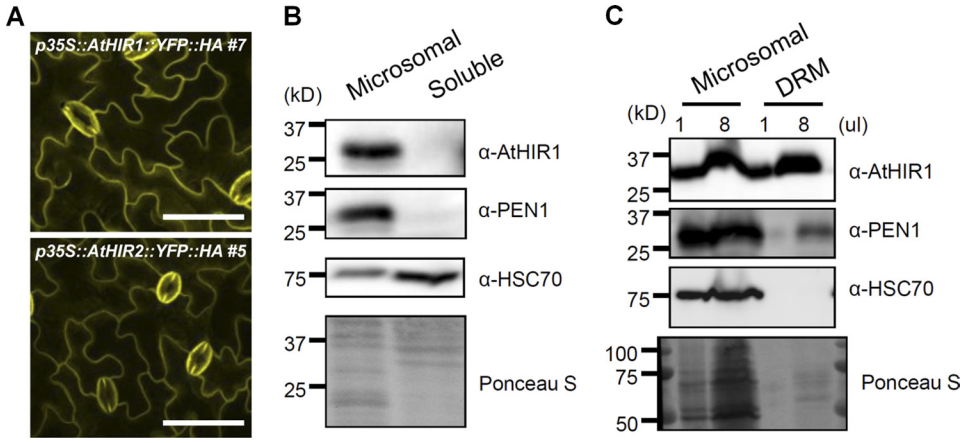

FIGURE 2. **AtHIR proteins are enriched in membrane microdomains of the PM.** *A,* AtHIR1 and AtHIR2 appear to be PM proteins. Representative YFP fluorescence images of both *p35S-AtHIR1-YFP-HA #7* and *p35S-AtHIR2-YFP-HA #5* T2 transgenic plants are shown. The *bars* indicate 100 μm. *B,* AtHIRs are membrane proteins. Total protein was extracted and fractionated into microsomal and soluble fractions. Protein samples from both microsomal and soluble fractions were analyzed by immunoblot using anti-AtHIR1 (*α-AtHIR1*), anti-PEN1 (*α-PEN1*), or anti-HSC70 (*α-HSC70*) antibodies. Total proteins transferred to a PVDF membrane were also visualized by Ponceau S staining. *C,* AtHIR proteins are enriched in detergent-resistant microdomains. One or 8 μl of a microsomal protein sample and a DRM protein sample were analyzed in a similar manner as in *B*. These experiments were performed twice independently with similar results.

Interestingly, two types of FRET signals were detected in different cells. The first type of FRET signal was detected all along the PM (Fig. 1*D*), and the second type had a punctate pattern along the PM as if it is restricted to certain PM microdomains (Fig. 1*E*). We could not identify the cause of these two distinct FRET patterns. Nevertheless, the locations of FRET signals suggest that AtHIR1-RPS2 complexes are present on the PM and are sometimes specific to certain PM microdomains. We could not detect FRET signals for the AtHIR2-CFP-HA and RPS2-YFP-HA pair, although both proteins were well expressed (data not shown). This implied that the way AtHIR2 formed a protein complex with RPS2 might be different from AtHIR1. These proteins did behave differently in other assays. For example, expression of AtHIR2, not AtHIR1, in *N. benthamiana* resulted in SDS-, 2-mercaptoethanol-, and heat-resistant oligomers (Fig. 1, *B* and *C*, and supplemental Fig. S2).

Enrichment of AtHIR Proteins in PM Microdomains—The FRET results suggest a PM localization of the RPS2-AtHIR complexes. To determine the subcellular localization of AtHIR proteins in general (not all AtHIR proteins may be in the complexes), confocal microscopy was performed using *p35S-AtHIR1-YFP-HA* and *p35S-AtHIR2-YFP-HA* transgenic plants, where both *AtHIR1* and *AtHIR2* were driven from a constitutive CaMV*35S* promoter (*p35S*). Both AtHIR1-YFP-HA and AtHIR2-YFP-HA appeared to be PM proteins (Fig. 2*A*). We tested the other two AtHIR proteins and found AtHIR3-YFP-HA and AtHIR4-YFP-HA also appeared to localize to PM (supplemental Fig. S3, *A* and *B*), which was further confirmed by plasmolysis (supplemental Fig. S3, *C* and *D*). To verify these observations, total protein extract from Col plants was fractionated into soluble and membrane fractions. Samples of both fractions were examined by immunoblot with anti-HIR1, anti-PEN1, and anti-HSC70 antibodies. Anti-PEN1 antibody specifically recognizes PEN1/SYP121 in *Arabidopsis* (47, 53). Like PM protein PEN1 (53), AtHIR proteins were only detected in the membrane fraction, suggesting that AtHIR proteins are localized to PM (Fig. 2*B*). In contrast, proteins recognized by anti-HSC70 were mainly localized to the soluble fraction (Fig. 2*B*), consistent with the known solubility of HSC70 (42).

Membrane microdomains enriched in sphingolipids and structural sterols, or "lipid rafts," are typically isolated as detergent (Triton X-100)-resistant membrane microdomains (DRMs) (46, 54–57). The observation that RPS2 complexes with AtHIR1 at specific PM sites (Fig. 1*E*) suggested that *Arabidopsis* HIR proteins may be present in membrane microdomains. To determine whether AtHIR proteins are localized to PM microdomains, DRMs were prepared from a microsomal fraction and subjected to immunoblot. The anti-HSC70 antibody detected some HSC70 isoforms in the microsomal fraction but not in the DRM fraction (Fig. 2*C*), suggesting that some HSC70 proteins are localized to membranes but are not enriched in DRMs. The anti-AtHIR1 antibody detected a band in the DRM fraction (Fig. 2*C*), suggesting that at least one member of AtHIR1, AtHIR2, and AtHIR4 is enriched in PM microdomains. The soluble NSF attachment protein receptor protein PEN1 was also detected in DRM fraction (Fig. 2*C*), which is consistent with previous reports that PEN1 may be present in PM microdomains (58, 59).

Homo-oligomerization of AtHIR Proteins—The observed homo-oligomer-like bands for AtHIR2 and AtHIR4 led us to investigate the ability of AtHIR proteins to form homo-oligomers *in vivo*. For testing homo-oligomerization, the same AtHIR protein was tagged at the C terminus with different epitope tags: the HPB tag (35) or the Myc tag. Pulldown assays using the *N. benthamiana* transient expression system were conducted. If the AtHIR proteins can form oligomers, oligomer complexes containing both AtHIR-HPB and AtHIR-Myc should be detected. As shown in Fig. 3*A*, AtHIR1-Myc was pulled down by AtHIR1-HPB when AtHIR1-HPB was co-expressed. No AtHIR1-Myc was pulled down by the streptavidin beads without co-expression of AtHIR1-HPB. Similar results were obtained for AtHIR2, AtHIR3, and AtHIR4 (Fig. 3*A*). Thus, each of the four AtHIR proteins can form homo-oligomers *in vivo*. Note that DSP cross-linking was not used in this

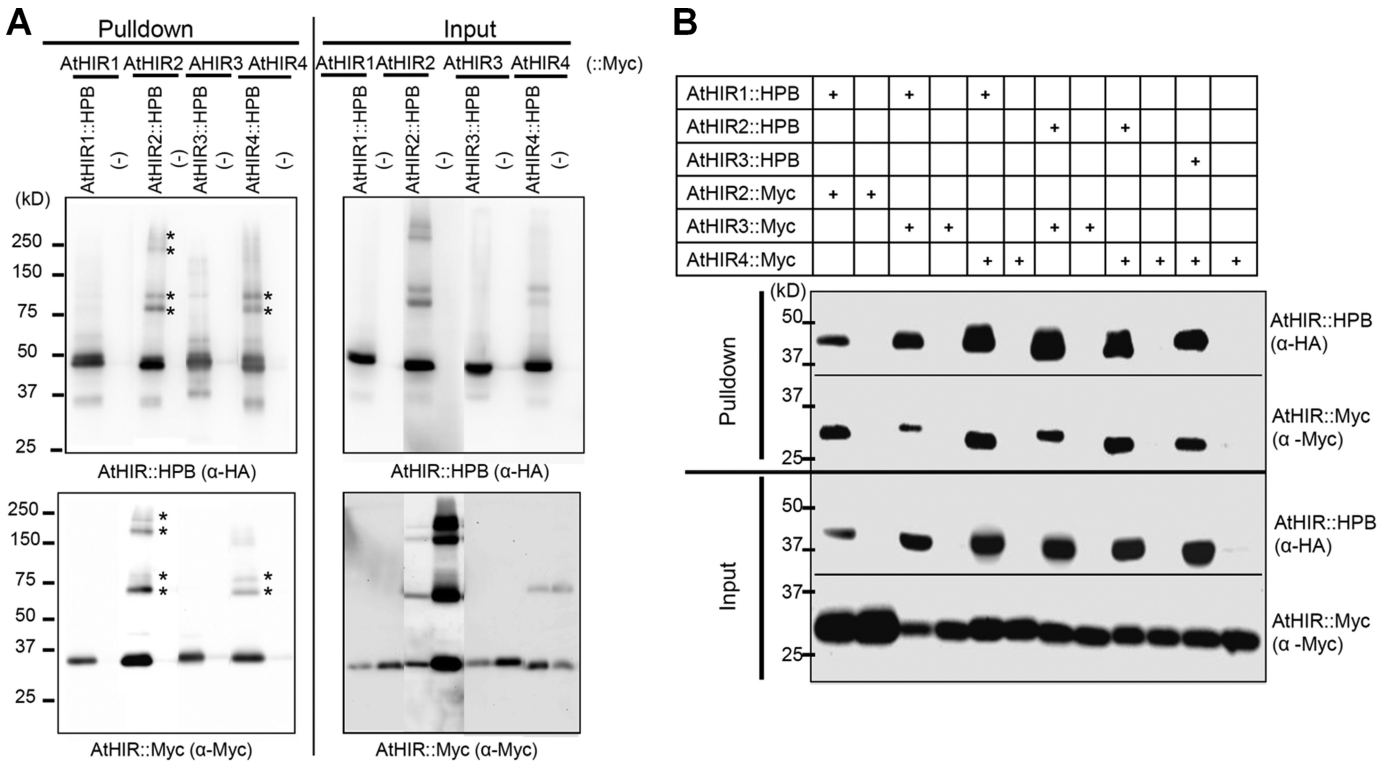

FIGURE 3. **Oligomerization of AtHIR proteins.** *A,* homo-oligomerization of AtHIR proteins in *N. benthamiana*. The AtHIR1/2/3/4 proteins were fused to either the Myc or HPB tags at their C termini. Both tagged versions of each AtHIR protein were co-expressed in a half-leaf of *N. benthamiana*. Only Myc-tagged AtHIR proteins were expressed in the other half of the leaf as negative controls. Total proteins were extracted and subjected to a pulldown using streptavidin beads. Both pulldown and input samples were analyzed by immunoblot using anti-HA (*α-HA*) and anti-Myc (*α-Myc*) antibodies. *B,* hetero-oligomerization of AtHIR proteins in *N. benthamiana*. Myc-tagged AtHIR2, AtHIR3, or AtHIR4 were co-expressed with HPB-tagged AtHIR1, AtHIR2. or AtHIR3 in a half-leaf of *N. benthamiana*, for detection of all six pairwise interactions. For negative controls, only Myc-tagged AtHIR proteins were expressed in the other half-leaf. Both pulldown samples and input samples were analyzed by immunoblot using anti-HA and anti-Myc antibodies. Protein bands representing SDS-, 2-mercaptoethanol-, and heat-resistant oligomers are indicated by *asterisks*. Both experiments were performed twice independently with similar results.

assay for AtHIR homo-oligomerization. SDS-, 2-mercaptoethanol-, and heat-resistant bands of large protein complexes containing AtHIR2 and AtHIR4 were detected in both pulldown and input samples. Apparent dimers consisting of either AtHIR2-HPB and AtHIR2-HPB or AtHIR2-HPB and AtHIR2-Myc were detected as distinct bands by immunoblot using anti-HA antibody due to their different molecular sizes (indicated by asterisks; compare the band sizes with those in Fig. 1*C*). A similar phenomenon was also observed for AtHIR4 (Fig. 3*A*).

Hetero-oligomerization of AtHIR Proteins—Because AtHIR proteins share high homology, we hypothesized that they may also form hetero-oligomers. To get a comprehensive view, all six possible pairwise combinations among the four AtHIR proteins were examined. The six tested pairs were as follows: AtHIR1-HPB and AtHIR2-Myc; AtHIR1-HPB and AtHIR3-Myc; AtHIR1-HPB and AtHIR4-Myc; AtHIR2-HPB and AtHIR3-Myc; AtHIR2-HPB and AtHIR4-Myc; and AtHIR3-HPB and AtHIR4-Myc. The pulldown assays for protein-protein interaction were performed similarly to test homo-oligomerization (no DSP cross-linking). All the pairwise interactions were detected (Fig. 3*B*), suggesting that the four AtHIR proteins could form hetero-oligomers in all possible combinations *in vivo*.

Induction of AtHIR Genes by Pto DC3000 and flg22—Many genes involved in disease resistance are pathogen-inducible. To examine whether the *Arabidopsis* AtHIR proteins are induced by infection with *P. syringae* strains, Col wild-type plants were inoculated with *Pto* DC3000 AvrRpm1, *Pto* DC3000 AvrRpt2, *Pto* DC3000, and *Pto* DC3000 *hrcC* strains. All the strains trigger the PTI response, but only the first three deliver type III effector proteins into the plant cell to interfere with PTI (12, 60). *Pto* DC3000 *hrcC* is deficient in the type III secretion system. It is not known whether *Pto* DC3000 can trigger some level of ETI response in Col plants. It is clear that *Pto* DC3000 AvrRpm1 and *Pto* DC3000 AvrRpt2 strains trigger strong ETI responses mediated by RPM1 and RPS2 in Col plants. These four different strains provide different plant-pathogen interaction conditions. With the bacterial dosage used here, *Pto* DC3000 AvrRpm1 normally triggers HR 6 h post-inoculation and *Pto* DC3000 AvrRpt2 triggers HR at a later time but within 24 h. We took time points up to 6 h post-inoculation for both *Pto* DC3000 AvrRpm1 and *Pto* DC3000 AvrRpt2. In both cases, modest induction of AtHIR proteins was detected by immunoblot using the anti-AtHIR1 antibody, at the early time points (Fig. 4*A*). With *Pto* DC3000 and *Pto* DC3000 *hrcC*, dramatic induction of AtHIR proteins was detected at 24 h post-inoculation (Fig. 4*A*). Because the induction levels of HIR proteins by the ETI strains (*Pto* DC3000 AvrRpm1 and *Pto* DC3000 AvrRpt2) were not noticeably higher than those by the PTI strains (*Pto* DC3000 and *Pto* DC3000 *hrcC*), we concluded that at least some AtHIR proteins are induced by MAMPs.

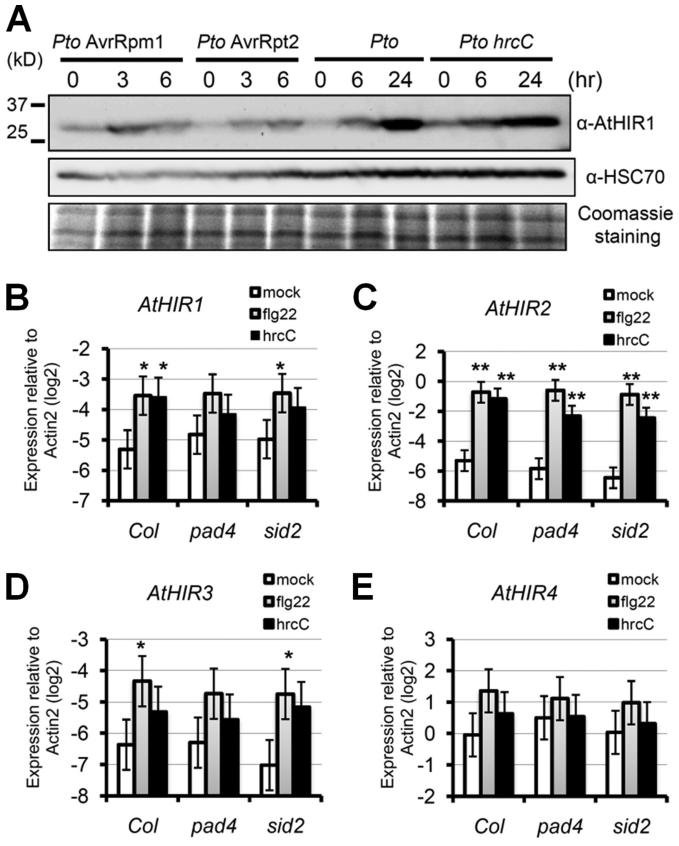

FIGURE 4. **Induction of *AtHIR* genes by *Pto* DC3000 strains and MAMPs.** *A,* induction of AtHIR proteins by *Pto* DC3000 strains. Five-week-old Col plant leaves were infiltrated with *Pto* DC3000 AvrRpm1 (*Pto* AvrRpm1), *Pto* DC3000 AvrRpt2 (*Pto* AvrRpt2), *Pto* DC3000 (*Pto*), or *Pto* DC3000 *hrcC* (*Pto hrcC*) at an inoculation dose of 1×10^8 colony formation units (CFU)/ml. Leaf samples were collected at the indicated time points. Total proteins were extracted and analyzed by immunoblot using anti-AtHIR1 antibody (α-*AtHIR1*). Blotting of HSC70 proteins using an anti-HSC70 antibody (α-*HSC70*) and Coomassie Brilliant Blue staining of part of the gel was used as loading controls. This experiment was performed three times independently with similar results. *B,* induction of *AtHIR* genes by flg22 and *Pto* DC3000 *hrcC* in Col, *pad4,* and *sid2*. The mRNA levels of *AtHIR1* (*B*), *AtHIR2* (*C*), *AtHIR3* (*D*), and *AtHIR4* (*E*) were determined by quantitative RT-PCR. The *vertical axis* represents the $\log_2$-transformed mRNA level relative to Actin2. The data were collected in three independent experiments and analyzed by a mixed linear model. The *bars* represent the means ± S.E. Significant differences compared with mock treatment are indicated by *asterisks* for $p < 0.1$ (*) and $p < 0.01$(**).

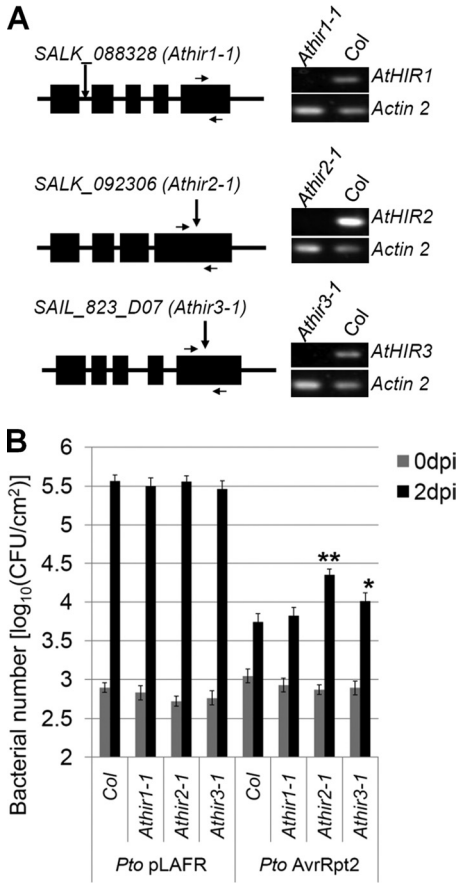

FIGURE 5. **Resistance to *Pto* DC3000 AvrRpt2 is compromised in *Athir2* and *Athir3* mutants.** *A,* T-DNA insertion mutants of *AtHIR1*, *AtHIR2*, and *AtHIR3* seem to be null. The *left panels* are schematic representations of the exon-intron structures of *AtHIR1* (*At1g69840*), *AtHIR2* (*At3g01290*), and *AtHIR3* (*At5g51570*), with exons shown as *black boxes*. The T-DNA insertion sites are shown by *vertical arrows*. The positions of the primers used in RT-PCR are shown by *horizontal arrows*. The *right panels* show the RT-PCR results, where the RT-PCR-product of *Actin 2* was used as an internal reference. *B, Athir2-1* and *Athir3-1* mutants were more susceptible than Col to *Pto* DC3000 AvrRpt2. Leaves of 5-week-old plants were inoculated with *Pto* DC3000 pLAFR (*Pto pLAFR*) and *Pto* DC3000 AvrRpt2 (*Pto AvrRpt2*) at a dose of 2×10^5 CFU/ml. The bacterial counts were measured at 0 and 2 days post-inoculation (*dpi*). The data were collected in two independent experiments and analyzed using a mixed linear model. The *bars* represent the means ± S.E. Significant differences between mutants and Col are indicated by *asterisks* for $p < 0.05$ (*) and $p < 0.005$(**).

To determine which *AtHIR* genes are induced by MAMPs, quantitative RT-PCR was conducted to monitor the mRNA levels of all four *AtHIR* genes in Col, *pad4,* and *sid2* plants treated with flg22 or *Pto* DC3000 *hrcC*. The *SID2* gene encodes the salicylic acid biosynthesis enzyme isochorismate synthase and is important for plant defense to multiple pathogens (61), and the *PAD4* gene is critical for salicylic acid-dependent immunity as well as salicylic acid-independent immunity (62, 63). *AtHIR1* was statistically significantly induced by both flg22 and *Pto* DC3000 *hrcC* in Col, but only significantly induced by flg22 in *sid2* plants (Fig. 4*B*). *AtHIR3* had a similar induction pattern except that induction by *Pto* DC3000 *hrcC* in Col was not significant (Fig. 4*D*). No statistically significant induction of *AtHIR4* was observed in any treatment or genotype (Fig. 4*E*). There was great induction (~16-fold) of *AtHIR2* upon flg22 and *Pto* DC3000 *hrcC* treatment, and such induction was still evident in *pad4* and *sid2* mutants (Fig. 4*C*). Taken together, the mRNA levels of all *AtHIR* genes except *AtHIR4* were significantly induced by some MAMPs (flg22 and *Pto* DC3000 *hrcC*), and such induction did not seem to be strongly dependent on *SID2* or *PAD4*.

Compromised Disease Resistance to Pto DC3000 AvrRpt2 in Athir2 and Athir3 Mutants—Physical association of AtHIR proteins and RPS2 suggests that they are involved in RPS2-mediated ETI. To examine this, T-DNA insertion lines for *AtHIR* genes were obtained from the ABRC stock center, and lines homozygous for the insertion alleles were selected (Fig. 5*A*). One putative knock-out allele for each gene except *AtHIR4* was confirmed by loss of mRNA accumulation measured by RT-PCR (Fig. 5*A*). For an unknown reason, the T-DNA insertion line for *AtHIR4* still accumulated the *AtHIR4* mRNA and was thus not studied further (supplemental Fig. S4). The three mutants were named *Athir1-1*, *Athir2-1,* and *Athir3-1*, respectively (Fig. 5*A*). All three mutants were tested for RPS2-medi-

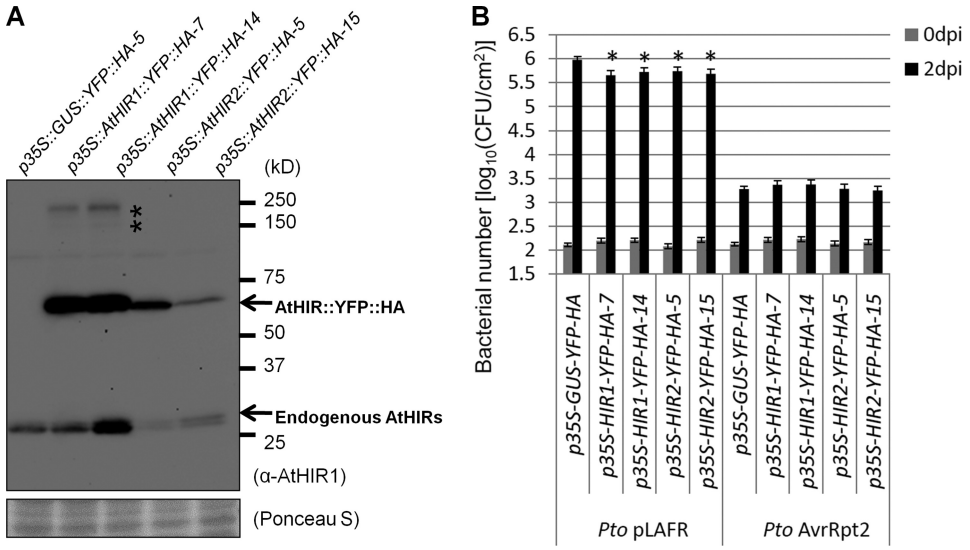

FIGURE 6. **Overexpression of *AtHIR1* and *AtHIR2* in *Arabidopsis* leads to enhanced resistance to *Pto* DC3000.** *A,* detection of YFP-HA-tagged AtHIR proteins by immunoblot. The *upper panel* shows immunoblot results using anti-HIR1 antibody. The *lower panel* shows Ponceau S staining of a part of the PVDF membrane as a loading control. YFP-HA-tagged AtHIR1 and AtHIR2 monomers are indicated by an *arrow*. Protein bands representing SDS-, 2-mercaptoethanol-, and heat-resistant oligomers (likely dimers and tetramers) are indicated by *asterisks*. One *GUS* line was used as a control. This experiment was performed twice independently with similar results. *B, AtHIR1* and *AtHIR2* overexpression lines show enhanced resistance to *Pto* DC3000. Five-week-old plants were inoculated with *Pto* DC3000 pLAFR (*Pto pLAFR*) or *Pto* DC3000 AvrRpt2 (*Pto AvrRpt2*) at the concentration of 2×10^5 CFU/ml. The bacterial counts were measured 0 and 2 days post-inoculation (*dpi*). The data were collected in three independent experiments and analyzed using a mixed linear model. Data from two *GUS* control lines were combined for analysis. The *bars* represent the means ± S.E. Significant differences compared with the bacterial counts in Col plants are indicated by *asterisks* for $p < 0.05$.

ated ETI using a bacterial growth assay. Growth of *Pto* DC3000 strains carrying an empty vector (pLAFR) or a construct encoding AvrRpt2 was compared between the mutants and wild-type plants. No difference was observed in the growth of *Pto* DC3000 pLAFR in the mutants compared with the wild type (Fig. 5*B*). However, there was significantly more growth of *Pto* DC3000 AvrRpt2 in *Athir2-1* and *Athir3-1* mutants than in the wild type (Fig. 5*B*). We cannot rule out the possibility that other unknown mutations in the insertion lines caused this phenotype because we did not test a second mutant allele for each gene. However, the fact that plant lines carrying mutations in two closely related genes exhibited a consistent phenotype strongly suggests that the mutations in *Athir2-1* and *Athir3-1* indeed cause the phenotype. Therefore, *AtHIR2* and *AtHIR3* genes play a positive role in RPS2-mediated ETI. There was no difference between *Athir1-1* and wild type for growth of *Pto* DC3000 AvrRpt2 (Fig. 5*B*).

Enhanced Disease Resistance to Pto DC3000 by Overexpressing AtHIR Genes—The effect of overexpressing *AtHIR1* and *AtHIR2* on resistance to *Pto* DC3000 was also tested. Two *AtHIR1* transgenic lines (*p35S-AtHIR1-YFP-HA-7* and *p35S-AtHIR1-YFP-HA-14*), two *AtHIR2* transgenic lines (*p35S-AtHIR2-YFP-HA-5* and *p35S-AtHIR2-YFP-HA-15*), and two control lines (*p35S-GUS-YFP-HA-3* and *p35S-GUS-YFP-HA-5*) were chosen for the study. YFP-HA-tagged AtHIR1 or AtHIR2 was detected in *HIR* overexpression lines, but not in the control line, by immunoblot using anti-HIR1 antibody (Fig. 6*A*). This time, SDS-, 2-mercaptoethanol-, and heat-resistant homo-oligomers were detected in *AtHIR1*-overexpression lines, but not in *AtHIR2*-overexpression lines (Fig. 6*A*), raising the possibility that such oligomers may result from high levels of overexpression. These transgenic lines were examined for growth of *Pto* DC3000 pLAFR and *Pto* DC3000 AvrRpt2. Two days after inoculation, reduced growth of *Pto* DC3000 pLAFR was observed in all four *HIR* overexpression lines when compared with the GUS control lines (Fig. 6*B*), indicating overexpression of *AtHIR1* or *AtHIR2* enhanced disease resistance to *Pto* DC3000. However, no difference in growth of *Pto* DC3000 AvrRpt2 was observed in these lines (Fig. 6*B*).

DISCUSSION

Our previous work identified AtHIR1 and AtHIR2 as putative RPS2 complex components (35). In this study, we confirmed that AtHIR1 and AtHIR2 are novel components of RPS2 complexes in both *Arabidopsis* and *N. benthamiana* (Fig. 1). The *N. benthamiana* transient expression system was used for rapid analysis. The proteins were likely overexpressed in the *N. benthamiana* experiments, which might result in artifactual physical associations. They corroborate results from stably transformed *Arabidopsis* plants in which the proteins were expressed from their natural promoters, strengthening this conclusion of complex formation. The involvement of AtHIR proteins in RPS2-mediated ETI was further supported by genetic analysis. Both *Athir2-1* and *Athir3-1* mutants show compromised resistance to *Pto* DC3000 AvrRpt2 but not to *Pto* DC3000 (Fig. 5*B*). This demonstrates that AtHIR2 and -3 proteins quantitatively contribute to RPS2-mediated ETI, presumably through their association with the RPS2 complex. The HIR gene family is conserved across many plant species (18–22, 64). Overexpression of the pepper CaHIR1 protein, which is most closely related to AtHIR4 among the four AtHIR proteins in *Arabidopsis*, led to spontaneous cell death (21), possibly suggesting activation of ETI signaling. Thus, it appears that plant HIR proteins generally play a positive role in ETI. Because the

leaky level of RPS2-mediated signaling in the absence of the effector AvrRpt2 is delicately balanced by the amounts of RIN4 and other proteins (14, 15, 65–69), it is conceivable that overexpression of a positive regulator of RPS2-mediated signaling, such as AtHIRs, leads to some level of constitutive activation of nonspecific immunity. This can provide a consistent explanation for both specific effects of *Athir2-1* and *Athir3-1* on RPS2-mediated ETI and enhancement of nonspecific immunity observed as enhanced immunity against *Pto* DC3000 by overexpression of AtHIR1 or AtHIR2 (Fig. 6). It was recently reported that *Arabidopsis* lines overexpressing a rice *HIR* gene also showed enhanced immunity against *Pto* DC3000 (70), which is consistent with our observation.

It is not known whether AtHIR proteins interact with RPS2 directly or indirectly through other protein(s) in the protein complexes. However, the very close physical association between AtHIR1 and RPS2 demonstrated by the FRET analysis (Fig. 1, *D* and *E*) strongly suggests a direct interaction between AtHIR1 and RPS2. CaHIR1 protein was shown to interact specifically with the LRR domain of CaLRR1 protein in a yeast two-hybrid assay (21). It was shown that the LRR domain of RPS2 determines specific interactions with host factors to confer RPS2-mediated immune response (71). It will be interesting to see whether AtHIR proteins specifically interact with the LRR domain of RPS2.

The SPFH domain-containing proteins have a propensity to form oligomers (25). For example, oligomerization has been reported with Stomatin (72), Podocin (73), Prohibitin (74, 75), and Reggies (76). Homo-oligomerization and hetero-oligomerization have been reported for different SPFH domain-containing proteins (29, 75, 77). Using pulldown assays, we found that all four AtHIR proteins could form homo-oligomers and hetero-oligomers when transiently expressed *in vivo* (Fig. 3). Furthermore, AtHIR1, AtHIR2, and AtHIR4 could form homo-oligomers that are resistant to SDS, 2-mercaptoethanol, and heat (Figs. 1*C*, 3, and 6 and supplemental Fig. S2), possibly as a consequence of overexpression. Hetero-oligomerization has been suggested to be necessary for stabilizing some SPFH domain-containing proteins (25). It will be interesting to know how homo- and hetero-oligomerization among the AtHIR proteins can affect their stability and function.

It is very common for SPFH domain-containing proteins to form small families with similar functions (25, 30). Three observations made in this study suggest AtHIR proteins function together. First, both AtHIR1 and AtHIR2 proteins form complexes with RPS2. Second, AtHIR proteins can form oligomers with all possible partners within the same family. Third, both *Athir2-1* and *Athir3-1* mutants showed defects in RPS2-mediated ETI, and overexpression of either *AtHIR1* or *AtHIR2* enhanced disease resistance to *Pto* DC3000. Although all four *AtHIR* genes are expressed in leaves, their abundance seems to be different (Fig. 4). When the amount of a mixture of AtHIR1, AtHIR2, and AtHIR4 proteins was measured by the anti-AtHIR1 antibody in Col, *Athir1-1*, and *Athir2-1* plants, a dramatic decrease of the AtHIR proteins was observed in *Athir2-1* (supplemental Fig. S5). As the anti-AtHIR1 antibody appears to recognize AtHIR1, AtHIR2, and AtHIR4 with similar affinities (supplemental Fig. S2, compare the results with the anti-Myc antibody), this immunoblot result indicates that AtHIR2 protein was the most abundant among the three. Furthermore, *AtHIR2* mRNA was the most MAMP-inducible of all the *AtHIR* mRNAs (Fig. 4). These observations suggesting that AtHIR2 is the dominant form of AtHIR in leaves are consistent with the observation that the *Athir2-1* mutant showed the most significant decrease in RPS2-mediated ETI (Fig. 5).

Although the SPFH domain-containing proteins in general have diverse subcellular distributions and different functions, they all have a common theme to their function, which is regulation of proteins in sterol-enriched membrane microdomains (25). SPFH domain-containing proteins are localized to various kinds of membrane systems and specifically enriched in microdomains of these membrane systems (25, 26, 29). Indeed, we found that all four AtHIR proteins were localized to the PM and at least some of them were enriched in the DRM, which is an operational definition of a membrane microdomain fraction (Fig. 2). Consistent with our observation, tobacco orthologs of AtHIR proteins were found in detergent-resistant PM fractions (78). AtHIR4 was found in a detergent-insoluble PM microdomain purified from *Arabidopsis* seedlings (79). Another proteomic study identified AtHIR1, AtHIR2, and AtHIR4 in a membrane microdomain fraction prepared from *Arabidopsis* callus (46). Recently, Choi *et al.* (64) showed that GFP-tagged CaHIR1 displayed punctate localization in the PM when it was expressed in onion epidermal cells. Such a punctate localization pattern in the PM is reminiscent of our FRET analysis results with AtHIR1 shown in Fig. 1*E*. The punctate localization patterns support the notion that HIR proteins reside in certain PM microdomains. Furthermore, Choi *et al.* (64) showed that the SPFH domain is sufficient for the CaHIR1 punctate localization pattern, suggesting that the SPFH domain of HIR proteins specifies localization to membrane microdomains. It will be interesting to investigate the molecular basis of AtHIR proteins' association to PM. For example, putative myristoylation sites were present in AtHIR1, AtHIR2, and AtHIR4 (supplemental Fig. S1*A*). If the HIR proteins are myristoylated, the myristoyl group may function as a lipid anchor to the PM.

What are the biological functions for formation of microdomains in plant PM? According to discussions about membrane microdomains in plants (46, 54, 58, 81, 82), such functions may include increasing focal protein concentration, promoting signal transduction, and facilitating exocytosis or endocytosis. These functions are not mutually exclusive. *Arabidopsis PEN1* encodes syntaxin SYP121, which is a component of the soluble NSF attachment protein receptor complex involved in vesicle fusion and exocytosis (53, 83). PEN1 plays a positive role in restricting fungal pathogen penetration in *Arabidopsis* (53). In this study, we showed that PEN1 was present in *Arabidopsis* PM microdomains (Fig. 2). The barley PEN1 homolog, HvROR2, was shown to be concentrated in membrane microdomain-like structures at fungal hyphal penetration sites (58), supporting the idea that membrane microdomain formation promotes exocytosis. Interestingly, knocking out both *PEN1* (*SYP121*) and its homolog *SYP122* activates multiple immune pathways (47, 84), suggesting PEN1 and SYP122-mediated exocytosis is critical in plant immunity. We demonstrated that some AtHIR proteins form protein complexes with

RPS2 and are involved in RPS2-mediated immunity, suggesting that membrane microdomains may play an important role in RPS2-mediated ETI. *AtHIR* genes are generally MAMP-inducible (Fig. 4), as is *RPS2* (5). Induction of both the *AtHIR* and *RPS2* genes through the PTI response may prime RPS2-mediated ETI. OsLRR1 and OsHIR1, rice homologs of CaLRR1 and CaHIR1, also interact with each other at the PM (85). It was shown that OsLRR1 underwent endocytosis when ectopically expressed in tobacco BY-2 cells (85). The SPFH domain-containing flotillins define a clathrin-independent endocytic pathway and mediate signaling from PM receptors to the cytoskeleton (25, 86). The *Arabidopsis* PTI receptor FLS2 undergoes endocytosis upon activation (87). We recently reported that FLS2 and RPS2 can reside in the same protein complex at the PM (88). It will be interesting to know whether such an endocytic phenomenon occurs with ETI receptors such as RPS2.

It has been well documented that bacterial pathogens and their products interact with membrane microdomains to promote entry into animal cells (89, 90). Such a phenomenon is difficult to imagine in plants due to the existence of strong cell walls. However, it is possible that *P. syringae* may require membrane microdomains on host PM to secrete effector proteins through the type III secretion system (TTSS). In fact, it was shown that formation of the TTSS needle-shaped structure for *Pseudomonas aeruginosa* was dependent on cholesterol (91), indicating membrane microdomains may play a role in allowing membrane disruption by TTSS. Another study showed that *P. aeruginosa* infection in human cells was dependent on sphingolipid-rich rafts (92). With the Gram-negative bacterial pathogen *Shigella flexneri*, it was further shown that purified detergent-resistant membranes could activate TTSS (93), demonstrating there is a membrane microdomain-based mechanism for contact-mediated secretion of bacterial effectors. A recent study suggested that oomycete and fungal pathogens deliver effector proteins to plant cells through membrane microdomain-mediated endocytosis (94). These observations strongly suggest that PM microdomains of the host cell are the point of effector delivery by many pathogens. Proteomic analysis of the DRM in rice and *Arabidopsis* revealed that many plant immunity-related proteins, including putative PTI and ETI receptors (80, 95), reside in the DRM, suggesting that membrane microdomains play an important role in pathogen recognition. We discovered that the membrane microdomain proteins AtHIRs play a positive role in RPS2-mediated ETI, likely through their physical association with RPS2. Conceivably, AtHIR proteins may increase the local concentration of RPS2, and possibly other R proteins, at PM microdomains to increase the detection sensitivity of pathogen effectors that are delivered at membrane microdomains.

Acknowledgments—We thank Jeff Dangl (University of North Carolina, Chapel Hill) for anti-RIN4 antibody and Mark Sanders and Tracy Anderson (College of Biological Sciences Imaging Center, University of Minnesota) for technical assistance on confocal imaging and FRET analysis.

REFERENCES

1. Ausubel, F. M. (2005) *Nat. Immunol.* **6,** 973–979
2. Jones, J. D., and Dangl, J. L. (2006) *Nature* **444,** 323–329
3. Tsuda, K., and Katagiri, F. (2010) *Curr. Opin. Plant Biol.* **13,** 459–465
4. Chinchilla, D., Bauer, Z., Regenass, M., Boller, T., and Felix, G. (2006) *Plant Cell* **18,** 465–476
5. Zipfel, C., Robatzek, S., Navarro, L., Oakeley, E. J., Jones, J. D., Felix, G., and Boller, T. (2004) *Nature* **428,** 764–767
6. Flor, H. H. (1971) *Annu. Rev. Phytopathol.* **9,** 275–296
7. Dangl, J. L., and Jones, J. D. (2001) *Nature* **411,** 826–833
8. Bent, A. F., Kunkel, B. N., Dahlbeck, D., Brown, K. L., Schmidt, R., Giraudat, J., Leung, J., and Staskawicz, B. J. (1994) *Science* **265,** 1856–1860
9. Mindrinos, M., Katagiri, F., Yu, G. L., and Ausubel, F. M. (1994) *Cell* **78,** 1089–1099
10. Grant, M. R., Godiard, L., Straube, E., Ashfield, T., Lewald, J., Sattler, A., Innes, R. W., and Dangl, J. L. (1995) *Science* **269,** 843–846
11. Warren, R. F., Henk, A., Mowery, P., Holub, E., and Innes, R. W. (1998) *Plant Cell* **10,** 1439–1452
12. He, P., Shan, L., and Sheen, J. (2007) *Cell. Microbiol.* **9,** 1385–1396
13. Chen, L. Q., Hou, B. H., Lalonde, S., Takanaga, H., Hartung, M. L., Qu, X. Q., Guo, W. J., Kim, J. G., Underwood, W., Chaudhuri, B., Chermak, D., Antony, G., White, F. F., Somerville, S. C., Mudgett, M. B., and Frommer, W. B. (2010) *Nature* **468,** 527–532
14. Mackey, D., Belkhadir, Y., Alonso, J. M., Ecker, J. R., and Dangl, J. L. (2003) *Cell* **112,** 379–389
15. Axtell, M. J., and Staskawicz, B. J. (2003) *Cell* **112,** 369–377
16. Greenberg, J. T. (1997) *Annu. Rev. Plant Physiol. Plant Mol. Biol.* **48,** 525–545
17. Greenberg, J. T., and Yao, N. (2004) *Cell. Microbiol.* **6,** 201–211
18. Nadimpalli, R., Yalpani, N., Johal, G. S., and Simmons, C. R. (2000) *J. Biol. Chem.* **275,** 29579–29586
19. Karrer, E. E., Beachy, R. N., and Holt, C. A. (1998) *Plant Mol. Biol.* **36,** 681–690
20. Rostoks, N., Schmierer, D., Kudrna, D., and Kleinhofs, A. (2003) *Theor. Appl. Genet.* **107,** 1094–1101
21. Jung, H. W., and Hwang, B. K. (2007) *Mol. Plant Pathol.* **8,** 503–514
22. Yu, X. M., Yu, X. D., Qu, Z. P., Huang, X. J., Guo, J., Han, Q. M., Zhao, J., Huang, L. L., and Kang, Z. S. (2008) *Gene* **407,** 193–198
23. Jung, H. W., Lim, C. W., Lee, S. C., Choi, H. W., Hwang, C. H., and Hwang, B. K. (2008) *Planta* **227,** 409–425
24. Tavernarakis, N., Driscoll, M., and Kyrpides, N. C. (1999) *Trends Biochem. Sci.* **24,** 425–427
25. Browman, D. T., Hoegg, M. B., and Robbins, S. M. (2007) *Trends Cell Biol.* **17,** 394–402
26. Morrow, I. C., and Parton, R. G. (2005) *Traffic* **6,** 725–740
27. Rivera-Milla, E., Stuermer, C. A., and Málaga-Trillo, E. (2006) *Cell. Mol. Life Sci.* **63,** 343–357
28. Hinderhofer, M., Walker, C. A., Friemel, A., Stuermer, C. A., Möller, H. M., and Reuter, A. (2009) *BMC Evol. Biol.* **9,** 10
29. Langhorst, M. F., Reuter, A., and Stuermer, C. A. (2005) *Cell. Mol. Life Sci.* **62,** 2228–2240
30. Browman, D. T., Resek, M. E., Zajchowski, L. D., and Robbins, S. M. (2006) *J. Cell Sci.* **119,** 3149–3160
31. Huber, T. B., and Benzing, T. (2005) *Curr. Opin. Nephrol. Hypertens.* **14,** 211–216
32. Mishra, S., Murphy, L. C., Nyomba, B. L., and Murphy, L. J. (2005) *Trends Mol. Med.* **11,** 192–197
33. Ahn, C. S., Lee, J. H., Reum Hwang, A., Kim, W. T., and Pai, H. S. (2006) *Plant J.* **46,** 658–667
34. Wang, Y., Ries, A., Wu, K., Yang, A., and Crawford, N. M. (2010) *Plant Cell* **22,** 249–259
35. Qi, Y., and Katagiri, F. (2009) *Plant J.* **57,** 932–944
36. Earley, K. W., Haag, J. R., Pontes, O., Opper, K., Juehne, T., Song, K., and Pikaard, C. S. (2006) *Plant J.* **45,** 616–629
37. Curtis, M. D., and Grossniklaus, U. (2003) *Plant Physiol.* **133,** 462–469
38. Mackey, D., Holt, B. F., 3rd, Wiig, A., and Dangl, J. L. (2002) *Cell* **108,** 743–754

39. Sessions, A., Burke, E., Presting, G., Aux, G., McElver, J., Patton, D., Dietrich, B., Ho, P., Bacwaden, J., Ko, C., Clarke, J. D., Cotton, D., Bullis, D., Snell, J., Miguel, T., Hutchison, D., Kimmerly, B., Mitzel, T., Katagiri, F., Glazebrook, J., Law, M., and Goff, S. A. (2002) *Plant Cell* **14,** 2985–2994
40. Tsuda, K., Sato, M., Glazebrook, J., Cohen, J. D., and Katagiri, F. (2008) *Plant J.* **53,** 763–775
41. Clough, S. J., and Bent, A. F. (1998) *Plant J.* **16,** 735–743
42. Qi, Y., Tsuda, K., Joe, A., Sato, M., Nguyen le V., Glazebrook, J., Alfano, J. R., Cohen, J. D., and Katagiri, F. (2010) *Mol. Plant Microbe Interact.* **23,** 1573–1583
43. Dangl, J. L., Ritter, C., Gibbon, M. J., Mur, L. A., Wood, J. R., Goss, S., Mansfield, J., Taylor, J. D., and Vivian, A. (1992) *Plant Cell* **4,** 1359–1369
44. Whalen, M. C., Innes, R. W., Bent, A. F., and Staskawicz, B. J. (1991) *Plant Cell* **3,** 49–59
45. Staskawicz, B., Dahlbeck, D., Keen, N., and Napoli, C. (1987) *J. Bacteriol.* **169,** 5789–5794
46. Borner, G. H., Sherrier, D. J., Weimar, T., Michaelson, L. V., Hawkins, N. D., Macaskill, A., Napier, J. A., Beale, M. H., Lilley, K. S., and Dupree, P. (2005) *Plant Physiol.* **137,** 104–116
47. Zhang, Z., Feechan, A., Pedersen, C., Newman, M. A., Qiu, J. L., Olesen, K. L., and Thordal-Christensen, H. (2007) *Plant J.* **49,** 302–312
48. Goodin, M. M., Zaitlin, D., Naidu, R. A., and Lommel, S. A. (2008) *Mol. Plant Microbe Interact.* **21,** 1015–1026
49. Jin, H., Axtell, M. J., Dahlbeck, D., Ekwenna, O., Zhang, S., Staskawicz, B., and Baker, B. (2002) *Dev. Cell* **3,** 291–297
50. Day, B., Dahlbeck, D., Huang, J., Chisholm, S. T., Li, D., and Staskawicz, B. J. (2005) *Plant Cell* **17,** 1292–1305
51. Hink, M. A., Bisselin, T., and Visser, A. J. (2002) *Plant Mol. Biol.* **50,** 871–883
52. Pollok, B. A., and Heim, R. (1999) *Trends Cell Biol.* **9,** 57–60
53. Collins, N. C., Thordal-Christensen, H., Lipka, V., Bau, S., Kombrink, E., Qiu, J. L., Hückelhoven, R., Stein, M., Freialdenhoven, A., Somerville, S. C., and Schulze-Lefert, P. (2003) *Nature* **425,** 973–977
54. Mongrand, S., Morel, J., Laroche, J., Claverol, S., Carde, J. P., Hartmann, M. A., Bonneu, M., Simon-Plas, F., Lessire, R., and Bessoule, J. J. (2004) *J. Biol. Chem.* **279,** 36277–36286
55. Jacobson, K., Mouritsen, O. G., and Anderson, R. G. (2007) *Nat. Cell Biol.* **9,** 7–14
56. Munro, S. (2003) *Cell* **115,** 377–388
57. Magee, A. I., and Parmryd, I. (2003) *Genome Biol.* **4,** 234
58. Bhat, R. A., and Panstruga, R. (2005) *Planta* **223,** 5–19
59. Kwon, C., Panstruga, R., and Schulze-Lefert, P. (2008) *Trends Immunol.* **29,** 159–166
60. Desveaux, D., Singer, A. U., and Dangl, J. L. (2006) *Curr. Opin. Plant Biol.* **9,** 376–382
61. Wildermuth, M. C., Dewdney, J., Wu, G., and Ausubel, F. M. (2001) *Nature* **414,** 562–565
62. Glazebrook, J., Zook, M., Mert, F., Kagan, I., Rogers, E. E., Crute, I. R., Holub, E. B., Hammerschmidt, R., and Ausubel, F. M. (1997) *Genetics* **146,** 381–392
63. Wang, L., Mitra, R. M., Hasselmann, K. D., Sato, M., Lenarz-Wyatt, L., Cohen, J. D., Katagiri, F., and Glazebrook, J. (2008) *Mol. Plant Microbe Interact.* **21,** 1408–1420
64. Choi, H. W., Kim, Y. J., and Hwang, B. K. (2011) *Mol. Plant Microbe Interact.* **24,** 68–78
65. Li, Y., Li, S., Bi, D., Cheng, Y. T., Li, X., and Zhang, Y. (2010) *PLoS Pathog.* **6,** e1001111
66. Holt, B. F., 3rd, Belkhadir, Y., and Dangl, J. L. (2005) *Science* **309,** 929–932
67. Takahashi, A., Casais, C., Ichimura, K., and Shirasu, K. (2003) *Proc. Natl. Acad. Sci. U.S.A.* **100,** 11777–11782
68. Tornero, P., Merritt, P., Sadanandom, A., Shirasu, K., Innes, R. W., and Dangl, J. L. (2002) *Plant Cell* **14,** 1005–1015
69. Austin, M. J., Muskett, P., Kahn, K., Feys, B. J., Jones, J. D., and Parker, J. E. (2002) *Science* **295,** 2077–2080
70. Zhou, L., Cheung, M. Y., Li, M. W., Fu, Y., Sun, Z., Sun, S. M., and Lam, H. M. (2010) *BMC Plant Biol.* **10,** 290
71. Banerjee, D., Zhang, X., and Bent, A. F. (2001) *Genetics* **158,** 439–450
72. Snyers, L., Umlauf, E., and Prohaska, R. (1998) *J. Biol. Chem.* **273,** 17221–17226
73. Huber, T. B., Simons, M., Hartleben, B., Sernetz, L., Schmidts, M., Gundlach, E., Saleem, M. A., Walz, G., and Benzing, T. (2003) *Hum. Mol. Genet.* **12,** 3397–3405
74. Back, J. W., Sanz, M. A., De Jong, L., De Koning, L. J., Nijtmans, L. G., De Koster, C. G., Grivell, L. A., Van Der Spek, H., and Muijsers, A. O. (2002) *Protein Sci.* **11,** 2471–2478
75. Tatsuta, T., Model, K., and Langer, T. (2005) *Mol. Biol. Cell* **16,** 248–259
76. Neumann-Giesen, C., Falkenbach, B., Beicht, P., Claasen, S., Lüers, G., Stuermer, C. A., Herzog, V., and Tikkanen, R. (2004) *Biochem. J.* **378,** 509–518
77. Huber, T. B., Schermer, B., Müller, R. U., Höhne, M., Bartram, M., Calixto, A., Hagmann, H., Reinhardt, C., Koos, F., Kunzelmann, K., Shirokova, E., Krautwurst, D., Harteneck, C., Simons, M., Pavenstädt, H., Kerjaschki, D., Thiele, C., Walz, G., Chalfie, M., and Benzing, T. (2006) *Proc. Natl. Acad. Sci. U.S.A.* **103,** 17079–17086
78. Morel, J., Claverol, S., Mongrand, S., Furt, F., Fromentin, J., Bessoule, J. J., Blein, J. P., and Simon-Plas, F. (2006) *Mol. Cell. Proteomics* **5,** 1396–1411
79. Shahollari, B., Vadassery, J., Varma, A., and Oelmüller, R. (2007) *Plant J.* **50,** 1–13
80. Keinath, N. F., Kierszniowska, S., Lorek, J., Bourdais, G., Kessler, S. A., Shimosato-Asano, H., Grossniklaus, U., Schulze, W. X., Robatzek, S., and Panstruga, R. (2010) *J. Biol. Chem.* **285,** 39140–39149
81. Martin, S. W., Glover, B. J., and Davies, J. M. (2005) *Trends Plant Sci.* **10,** 263–265
82. Grennan, A. K. (2007) *Plant Physiol.* **143,** 1083–1085
83. Bassham, D. C., and Blatt, M. R. (2008) *Plant Physiol.* **147,** 1504–1515
84. Zhang, Z., Lenk, A., Andersson, M. X., Gjetting, T., Pedersen, C., Nielsen, M. E., Newman, M. A., Hou, B. H., Somerville, S. C., and Thordal-Christensen, H. (2008) *Mol. Plant* **1,** 510–527
85. Zhou, L., Cheung, M. Y., Zhang, Q., Lei, C. L., Zhang, S. H., Sun, S. S., and Lam, H. M. (2009) *Plant Cell Environ.* **32,** 1804–1820
86. Glebov, O. O., Bright, N. A., and Nichols, B. J. (2006) *Nat. Cell Biol.* **8,** 46–54
87. Robatzek, S., Chinchilla, D., and Boller, T. (2006) *Genes Dev.* **20,** 537–542
88. Qi, Y., Tsuda, K., Glazebrook, J., and Katagiri, F. (2011) *Mol. Plant Pathol.* **12,** 702–708
89. Zaas, D. W., Duncan, M., Rae Wright, J., and Abraham, S. N. (2005) *Biochim. Biophys. Acta* **1746,** 305–313
90. Lafont, F., Abrami, L., and van der Goot, F. G. (2004) *Curr. Opin. Microbiol.* **7,** 4–10
91. Schoehn, G., Di Guilmi, A. M., Lemaire, D., Attree, I., Weissenhorn, W., and Dessen, A. (2003) *EMBO J.* **22,** 4957–4967
92. Grassmé, H., Jendrossek, V., Riehle, A., von Kürthy, G., Berger, J., Schwarz, H., Weller, M., Kolesnick, R., and Gulbins, E. (2003) *Nat. Med.* **9,** 322–330
93. van der Goot, F. G., Tran van Nhieu, G., Allaoui, A., Sansonetti, P., and Lafont, F. (2004) *J. Biol. Chem.* **279,** 47792–47798
94. Kale, S. D., Gu, B., Capelluto, D. G., Dou, D., Feldman, E., Rumore, A., Arredondo, F. D., Hanlon, R., Fudal, I., Rouxel, T., Lawrence, C. B., Shan, W., and Tyler, B. M. (2010) *Cell* **142,** 284–295
95. Fujiwara, M., Hamada, S., Hiratsuka, M., Fukao, Y., Kawasaki, T., and Shimamoto, K. (2009) *Plant Cell Physiol.* **50,** 1191–1200